Torque studies of large-area Co arrays fabricated by etched nanosphere lithography

S. M. Weekes[a] and F. Y. Ogrin
School of Physics, University of Exeter, Exeter, EX4 4QL, United Kingdom

(Presented on 11 November 2004; published online 12 May 2005)

Large-area arrays of size-tunable Co nanomagnets have been fabricated using a methodology based on nanosphere lithography. The technique employs a monolayer of latex spheres as an inverse mask for the formation of Co elements by electrodeposition. By tuning the size of the spheres with reactive ion etching, magnetic elements of 310 and 240 nm diameter have been obtained. Analysis of the arrays using high-field torque magnetometry and three-dimensional micromagnetic modeling clearly demonstrates a change in anisotropy as the diameter of the elements is reduced. More detailed investigation of the field dependence indicates the presence of magnetic vortices at low fields. © *2005 American Institute of Physics*. [DOI: 10.1063/1.1849665]

I. INTRODUCTION

Patterned magnetic nanostructures are currently the subject of much interest due to their enormous potential in future nanotechnology, including high density magnetic recording. Due to the low dimensions and increased stability of isolated elements, a move to patterned media could increase storage densities by ~100 times[1] compared to that currently available on computer hard drives. Despite the advantages of using patterned media, there are still challenges involved in the fabrication and characterization of patterned arrays. Many of the fabrication procedures which are currently in use, such as electron beam lithography, are costly and not suited to the production of arrays over large areas (1 cm^2 and above). However, large-area arrays are not only a prerequisite for magnetic recording applications but they are also essential for the detailed study of patterned media. In this investigation we use a fabrication technique, etched nanosphere lithography (ENL), which is cost effective, simple to implement and capable of producing large-area arrays with a range of dimensions.

ENL utilizes commercially available polystyrene (PS) nanospheres to create a hexagonal close-packed pattern of holes in a dielectric layer. The sphere diameter can be adjusted after deposition through reactive ion etching (RIE) facilitating the production of size-tunable magnetic arrays. ENL is thus a valuable tool in the fabrication of patterned arrays for magnetic studies. In this article, ENL has been used to produce Co arrays with element diameters of 310 and 240 nm. A preliminary analysis of the arrays has been performed using high-field torque magnetometry, along with three-dimensional (3D) micromagnetic simulations (OOMMF).[2] These results are compared to measurements made on an electrodeposited Co film of the same thickness as the arrays.

[a]Author to whom correspondence should be addressed; electronic mail: s.m.weekes@ex.ac.uk

II. FABRICATION

The fabrication procedure involved the following steps. A metallic layer of Cu was evaporated onto a glass substrate to create an electrode for the final stage electrodepositon. A further 200 nm of SiO_2 was then deposited on top of the metallic layer using rf sputtering. Nanospheres of 390 nm diameter were deposited onto the substrate by drop coating a mixture of Milli-Q water and solution containing PS spheres, in the ratio 14:1. After sphere deposition, the samples were dried in an enclosed atmosphere at 55 °C, resulting in the formation of large monolayers, typically of areas greater than 1 cm^2 [Fig. 1(a)]. RIE in an O_2 atmosphere was used to reduce the sphere diameter after deposition and thereby obtain elements of different diameters. After RIE, an etch mask of MgF_2 was evaporated onto the samples, covering the spheres and filling the recesses between them [Fig. 1(b)]. Removal of the spheres was achieved using alcohol, after which the pattern was transferred through the SiO_2 layer to reach the metallic electrode below using RIE in a CHF_3 atmosphere [Fig. 1(c)]. Finally, magnetic elements were grown

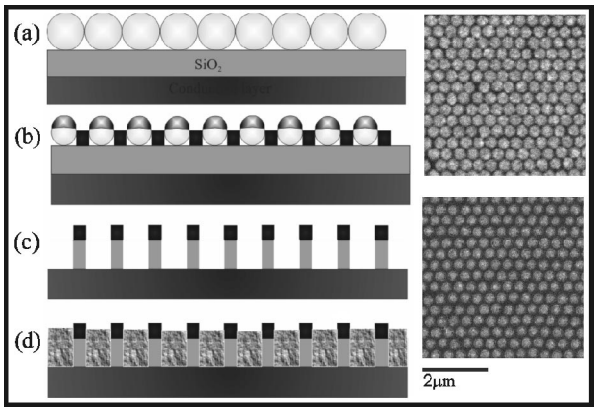

FIG. 1. Schematic diagram of the fabrication process. (a) Deposition of a monolayer of PS spheres. (b) Reduction of the sphere diameter using RIE and subsequent evaporation of MgF_2. (c) Removal of the spheres and RIE to leave an array of holes. (d) Electrodeposition of Co to form an array of columns. The inset shows SEM images of Co arrays of diameter 310 nm (above) and 240 nm (below).

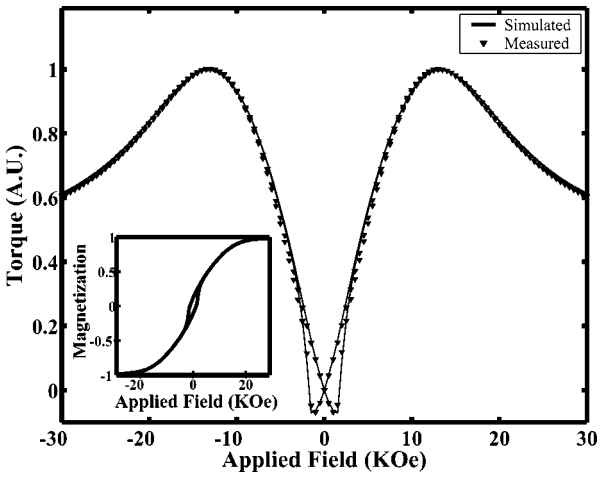

FIG. 2. Field dependent torque signal for a 260-nm-thick electrodeposited Co film with a magnetic field applied at 80° to the sample plane. The data are well represented by a coherent rotation model (solid line). The inset shows the simulated magnetization loop demonstrating hard axis behavior.

by electrodeposition in a Co sulphate bath [Fig. 1(d)]. Scanning electron microscopy (SEM) images of the fabricated arrays are shown in Fig. 1.

III. MAGNETIC MEASUREMENTS

A high-field torque magnetometer was used to analyze the magnetic properties of the arrays. Measurements were performed in two modes: (1) Angular Dependence, which involved rotating the sample in the plane of a fixed magnetic field but perpendicular to the plane of the sample. (2) Field Dependence, where the sample was maintained at a fixed angle while the magnetic field was swept between positive and negative values to complete a hysteresis loop. The surface normal of the sample defined the *z* direction and the field was applied in the *x*-*z* plane, while the torque in the *y* direction was measured.

Unlike the majority of magnetization techniques, which probe the component of magnetization in the field direction, torque magnetometry is sensitive to the component of magnetization perpendicular to the applied field, making it ideal for investigating anisotropic materials.[3] When analyzing the field dependent torque signal for a field applied close to perpendicular to the easy direction, one may consider two main features: First, the hysteretic region at low fields holds information related to the magneto-crystalline anisotropy, domain formation and inter-particle interactions that control switching. Second, the position of the turning point at high field holds information regarding the magnitude of the magnetic moment and the magnetostatic field, providing the latter is much larger than the crystalline anisotropy field. These features are considered in the following discussion.

IV. RESULTS AND DISCUSSION

A. Continuous Co film

Figure 2 shows the measured and simulated torque signal from a continuous Co film of thickness 260 nm produced by electrodeposition. The field was applied at 80° to the sample plane and swept between ±30 kOe. A Stoner–Wohlfarth model was used to simulate the field dependent signal. The Co film was assumed to be polycrystalline and was represented in the model as an ensemble of randomly oriented crystallites, each having uniaxial crystalline anisotropy. Although this type of analysis is an approximation as it does not include exchange coupling between crystallites, it is useful in that it allows magnetic parameters to be estimated in considerably less computing time than micromagnetic analysis. The simulation indicates that the Co film has very weak crystalline anisotropy with a magneto-crystalline anisotropy constant of $K \sim 0.4 \times 10^6$ erg cm^{-3}. This value is an order of magnitude lower than that for a perfect hcp Co crystal, and should be treated with caution due to the limitations of the model in the low-field region, where switching may not occur through uniform rotation. Nevertheless, exchange coupling and the surface anisotropy associated with small crystallites can have a significant affect on the measured value of K and other studies[4] have shown a similar reduction in crystalline anisotropy for electrodeposited Co. The value of the saturation magnetization extracted from the simulation was $M_s = 1200$ emu cm^{-3}, this is comparable to the bulk value[5] of 1422 emu cm^{-3}. The reduction in M_s is likely due to the presence of impurities in the electrodeposited film. Other investigations[6] of electrodeposited Co consistently found that the value of M_s was reduced to between 1100 and 1270 emu cm^{-3} due to the co-deposition of impurities.

B. Co arrays

In order to investigate the behavior of patterned arrays, torque measurements were supported by simulations using a 3D micromagnetic solver (OOMMF). The input parameters for bulk hcp Co were employed, with the exception of the saturation magnetization where a value of $M_s = 1200$ emu cm^{-3} was used, as extracted from the Co film measurement. The simulations were carried out over arrays of 5×5 elements using a cell size of 20 nm. The directions of the crystal easy axes were varied randomly from cell to cell to simulate the polycrystalline Co structure. Figure 3(a) shows both the field dependent and the angular dependent torque for patterned Co arrays of diameters 240 and 310 nm and thickness 260 nm. The angular dependent signal (inset), exhibits a hysteretic switching region at angles of 90° and 270° between the sample plane and the applied field, indicating a preferred in-plane easy direction.

The field dependent torque signal shown in Fig. 3(a) was obtained after applying a field at 80° to the sample plane and sweeping it between ±30 kOe. Comparison between the torque curves for the two samples highlights the following: (1) a large reduction in amplitude for the 240 nm array, even after allowing for the different volume of magnetic material present; (2) a shift of the turning points in the high-field region, from 10.5 kOe for the 310 nm array to 8.5 kOe for the 240 nm array; (3) a shallower torque gradient in the high-field region for the 240 nm array, indicating closer alignment with the applied field. These differences are all indications of a reduction in the in-plane anisotropy as the diameter of the elements is reduced. For example, the high-field turning

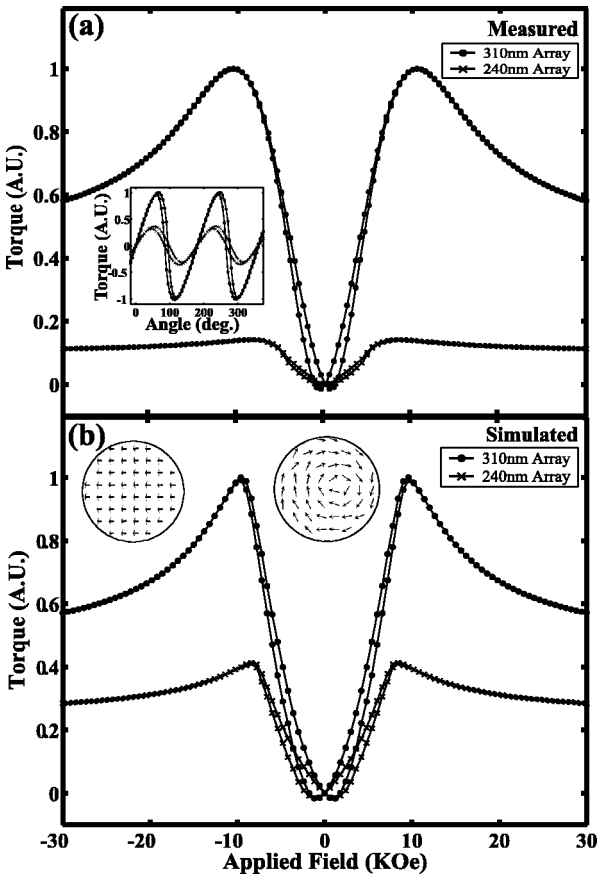

FIG. 3. (a) Measured field dependent torque signal for arrays of 310 and 240 nm diameter, with a field applied at 80° to the sample plane. The inset shows the angular dependent signal for an applied field of 3 kOe. The asymmetry of the curve indicates a preferred in-plane easy axis for both arrays. (b) Simulated torque signal using a 3D micromagnetic model. The simulations qualitatively reproduce the features seen in (a). The inset shows the calculated vortex state at remanence, (center) and the near saturated state at 30 kOe, (left).

point in the torque curve results from the interplay between the increasing field that acts to increase torque, and the alignment of the magnetization vector with the applied field which acts to decrease torque. For samples with reduced in-plane anisotropy the alignment of the magnetization vector occurs at lower fields thereby shifting the turning point. Similarly, the reduction in the overall amplitude of the signal and the reduced gradient at high fields are both indicators of a decrease in the in-plane component of magnetization. This change in anisotropy is likely due to a combination of the change in aspect ratio and the reduction of the inter-element dipolar field as the element diameter is reduced.

Micromagnetic simulations qualitatively reproduce all of the above features, as seen in Fig. 3(b). While simulations show a marked reduction in the overall torque amplitude for the 240 nm array, the reduction is not as large as that seen in the experimental data. This may be an indication that the cumulative effect of inter-element magnetostatic interactions in the large-area sample is not well accounted for in simulations performed over an array of only 5×5 elements. Simulations also indicate the presence of magnetic vortices in the low-field region [Fig. 3(b) inset]. Due to their low dimensions, each element accommodates a single vortex with the exact position of the vortex core within the element, dependent on the element's position within the array. This vortex structure is seen for fields below 8.4 and 7.6 kOe for the 310 and 240 nm arrays, respectively, indicating greater stability against vortex formation for smaller elements.

Comparison between the patterned arrays and the continuous Co film (Fig. 2) in the low-field region highlights a more diffuse hysteresis in the patterned arrays, indicating incoherent switching of the elements over a range of field values. This incoherent switching is an indication that the elements within the array have a distribution of switching fields. In contrast to the continuous Co film, the patterned samples feature arrays of exchange decoupled elements. Previous studies[7] have shown that this can result in a distribution of switching fields due to the local environment produced by magnetostatic interactions. Simulations of the patterned arrays show a similarly diffuse, although broader, hysteretic switching region. Differences between the simulated and experimental data in this region likely arise from the difficulty in accurately representing the magnetic anisotropy present in polycrystalline samples.

V. CONCLUSION

Torque magnetometry has been used to investigate the anisotropic properties of Co arrays revealing a change in anisotropy as the element diameter is reduced. Comparisons with measurements made on a continuous Co film point to incoherent switching of the elements. These conclusions are supported by 3D micromagnetic simulations, which also show the presence of magnetic vortices at low fields. This investigation has demonstrated the sensitivity of torque measurements to changes in anisotropy, even for a very modest increase in aspect ratio, (height/diameter=0.8 for the 310 nm elements and 1.1 for the 240 nm elements). Further work will use torque magnetometry along with the ENL fabrication technique to probe the transition to a perpendicular ground state as the aspect ratio of the elements is increased.

[1]S. Sun, C. B. Murray, D. Weller, L. Folks, and A. Moser, Science **287**, 1989 (2000).
[2]M. J. Donahue and D. G. Porter, NISTIR 6376, National Institute of Standards and Technology, 100 Bureau Drive, Gaithersburg, MD 20899, 1999.
[3]R. Hohne, C. A. Kleint, A. V. Pan, M. K. Krause, M. Ziese, and P. Esquinazi, J. Magn. Magn. Mater. **211**, 271 (2000).
[4]C. A. Ross, M. Hwang, and M. Shima *et al.*, Phys. Rev. B **65**, 144417 (2002).
[5]H. P. Myers and W. Sucksmith, Proc. R. Soc. London, Ser. A **207**, 427 (1951).
[6]C. A. Ross, M. Hwang, and M. Shima *et al.*, J. Magn. Magn. Mater. **249**, 200 (2002).
[7]J. I. Martin, J. Noguesb, K. Liu, J. L. Vicent, and I. K. Schuller, J. Magn. Magn. Mater. **256**, 449 (2003).